



Cite this: *CrystEngComm*, 2015, 17, 7227

Crystallization of triple- and quadruple-stranded dinuclear bis- β -diketonate-Dy(III) helicates: single molecule magnetic behavior†

Peng Chen,^a Hongfeng Li,^a Wenbin Sun,^a Jinkui Tang,^{*b} Lei Zhang^a and Pengfei Yan^{*a}

Helical structures are vital in chemistry and biochemistry and their importance has been reconsidered since the structure of DNA was revealed. Over the past decades, the advantages of the helical structures of bis- β -diketonate-based multiple-stranded Ln³⁺ complexes have been speculated with respect to their unique structures. Based on our previous study, we have designed a V-shaped bis- β -diketone ligand, H₂MBDA, which has been utilized to crystallographically synthesize triple-stranded and quadruple-stranded dinuclear Dy³⁺ complexes. In contrast to the absence of crystallographical results in previous studies, the successful crystallization in this study has contributed to the functionalization of the -CF₃ groups into the ligand as the termini, which have played a key role in the crystallization through intermolecular weak interactions. Both complexes display slow magnetic relaxation. The auxiliary ligand, phenanthroline, contributes to both tuning the structure and strengthening the anisotropy barrier.

Received 2nd June 2015,
Accepted 12th August 2015

DOI: 10.1039/c5ce01067e

www.rsc.org/crystengcomm

Introduction

The self-assembly of lanthanide compounds with desired functional groups and controlled structural motifs has been the subject of many studies,¹ whereas helices have been the focus with respect to their simplicity and significance as the basic structural motif in chemistry and biochemistry.² Besides geometrical remarks, intriguing magnetic and luminescent behaviors have been revealed with nonequivalent *g*-tensor and improved sensitivity, respectively.³ Moreover, various ligands with different lengths and sequences have been designed in the pursuit of multiple-stranded helicates,⁴ and Piguet and Bünzli have greatly contributed to developments in this field.^{1g,2b,f,5}

β -Diketones as versatile ligands are qualified to ligate to lanthanide ions, and bis- β -diketones have recently been utilized to construct multiple-stranded helicates.^{4f} Pikramenou has shown the advantages of multiple-stranded helicates in enhancing emission with a higher quantum yield,⁶ but the proposed

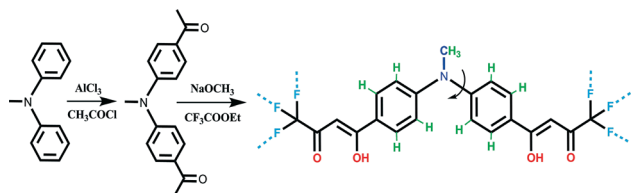
multiple-stranded complexes were not crystallographically characterized.⁷ The absence of crystallographical evidence has stemmed further studies on the relationship between structure and property. Over the past decade, many advances have been achieved in the design of the ligands, but the examples of lanthanide helicates assembled with bis- β -diketones are rare. The crystallization of such helical structures comprises coordination interactions between ligands and metal centers as well as subtle control of intermolecular interactions between helical units.^{2f,5,8} Less consideration of the intermolecular interactions results in poor crystallization of bis- β -diketonate-Ln³⁺ helicates, while most solution-based studies have concluded that a combination of rigidity, length and flexibility of the ligand is responsible for the coordination interactions.⁹ On account of previous aspects of the crystallization of lanthanide helicates and structural features in the crystallization of triple-stranded helicates in our previous study,^{2f,8} the -CF₃ groups are introduced to enrich and strengthen the intermolecular interactions and to facilitate the crystallization of bis- β -diketone-based helicates. In addition, the multiple-stranded, bridged, dinuclear lanthanide systems, featured in the similar coordination environment of the Dy³⁺ center, could provide a way to tune the anisotropy axes to align the anisotropic axis with a higher energy barrier for spin reversal.^{3a}

Herein, we present the syntheses and crystallization of triple-stranded and quadruple-stranded helicates assembled about a V-shaped bis- β -diketone ligand, *N*-methyl-4,4'-bis(4,4,4-trifluoro-1,3-dioxobutyl)diphenylamine (H₂MBDA) (Scheme 1).

^a Key Laboratory of Functional Inorganic Material Chemistry (MOE), School of Chemistry and Materials Science, Heilongjiang University, Harbin 150080, PR China. E-mail: yanpf@vip.sina.com

^b State Key Laboratory of Rare Earth Resource Utilization, Changchun Institute of Applied Chemistry, Chinese Academy of Sciences, Changchun 130022, PR China. E-mail: tang@ciac.ac.cn

† Electronic supplementary information (ESI) available: Full experimental procedures, NMR, crystallographical information and magnetic data. CCDC: 1054122-4. For ESI and crystallographic data in CIF or other electronic format see DOI: 10.1039/c5ce01067e



Scheme 1 Synthetic route for the ligand H₂MBDA and the schematic representation of the potential functionalization in the ligand (black: the rigid and lengthy spacers that separate the binding units; red: the binding sites that allow coordination to Dy³⁺ ions; blue: the *N*-methyl group that undergoes helication and avoids the formation of mesocates; green and light blue: H atoms and –CF₃ groups that exhibit weak C–H⋯F and F⋯F interactions).

The coordination of four ligands to two Dy³⁺ ions at the termini gives rise to the formation of quadruple-stranded **1**, whereas the employment of three ligands leads to the formation of a triple-stranded helicate **2** in addition to two phenanthroline (phen) molecules. Interestingly, single molecular magnet (SMM) behavior is observed for **2** with respect to the slow relaxation of **1** under zero dc field, which is ascribed to the incorporation of phen as the auxiliary ligand in **2**.¹⁰

Results and discussion

Structural analysis revealed that **1** crystallizing in the monoclinic space group of *C2/c* is a quadruple-stranded dinuclear helicate (Fig. 1). Each crystallographically distinct Dy³⁺ ion is eight-coordinated to O atoms from four MBDA ligands in a square antiprism geometry. The Dy–O bond lengths are in the range of 2.359(4)–2.433(4) Å, which are in accordance with the reported values. The geometry of each Dy³⁺ center is slightly different and detailed bond lengths are presented in Table S2.† A cavity is therefore formed by four deprotonated ligands that wrap around two Dy³⁺ ions in a helical fashion,

where a diethyl ether molecule is captured during the crystallization. The dihedral angles between the two phenyl groups in each MBDA ligand are in the range of 56.6(2)–66.4(2)°, indicative of the ability to twist. The negative charge of [Eu₂(MBDA)₄]^{2–} is balanced by the protonated triethylamines. The Dy⋯Dy distance in the same helicate is 12.6 Å, which is comparable to that in the triple-stranded Eu₂(BTB)₃.^{8a}

Having validated the crystallization of the quadruple-stranded helicate **1**, we target an alternative strategy for the preparation of the triple-stranded helicate **2** through the incorporation of neutral phen molecules. **2** crystallizing in the triclinic space group of *P1̄* is a triple-stranded dinuclear helicate. Each crystallographically independent Dy³⁺ ion is also eight-coordinated to six O and two N atoms from three MBDA ligands and one phen in a square antiprism geometry. The Dy–O and Dy–N bond lengths are in the range of 2.277(2)–2.374(2) Å and 2.531(2)–2.573(3) Å, respectively. Similarly, three interwinding MBDA ligands around two Dy³⁺ centers result in the helical structure of **2**. The dihedral angles between the two phenyl groups in each MBDA are in the range of 51.8(10)°–60.3(1)°. The Dy⋯Dy distance of 13.4 Å in **2** is slightly longer than that of **1**, and it is long enough to exclude intramolecular magnetic coupling in both cases.

Obviously, understanding the factors affecting crystal engineering would be a significant task for the synthesis of functional materials,¹¹ and it would provide deeper insight into the supramolecular assembly as well as the functional behavior arising from the host–guest chemistry.¹² With respect to the crystallization of triple-stranded helicates based on bridging ligands containing two –CF₃ termini, we believe that some points are worth considering with respect to the syntheses of the potential bis-β-diketone ligands for the crystallization of quadruple-stranded helicates. First, the rigid and lengthy moieties in the backbone enable them to sufficiently form strands and chelate to two distinct metal ions (Scheme 1). With respect to the twisting plight of BTB in Eu₂(BTB)₃, flexibility is a primary requirement for the ligand to form the potential quadruple helicates, and an *N*-methyl group is therefore inserted between the two phenyl moieties.

In fact, this allows MBDA to twist around, adopting a wide range of conformations; moreover, its asymmetric nature helps to avoid the formation of mesocates.¹³ However, its flexibility permits the ligands to settle into various conformations, disturbing the inter-ligand stacking. In respect to the reported results, the successful crystallization may lie in the weak interactions, which always play a substantial role in driving the self-assembly. Finally, the –CF₃ groups at the termini have been functionalized into a ligand in which fluorine has structural significance in the crystal engineering.¹⁴ As expected, extensive C–H⋯F and F⋯F interactions are detected for **1** and **2**, which steer the molecular orientation of the aromatic rings in the solid state.¹⁵ The numerous interactions allow the complexes to crystallize from the solution as a mixture of conformations¹⁶ because different conformers have been observed in **1** and **2**, resulting from the easy rotation about the C_{phenyl}–N single bond.

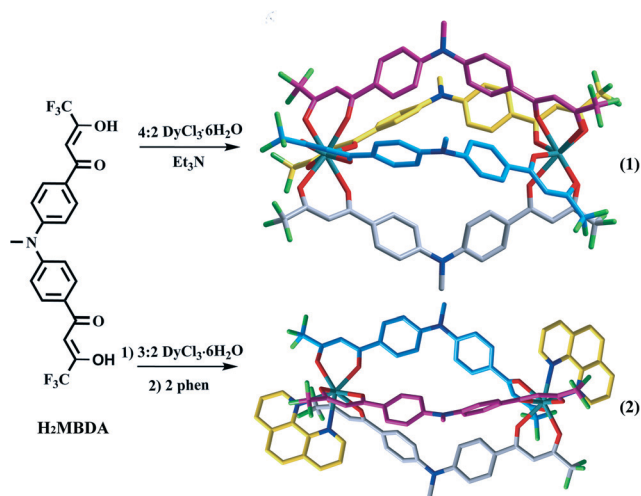


Fig. 1 The assemblies of quadruple-stranded **1** and triple-stranded **2** helicates. The C atoms in each ligand are marked in a different colour. H atoms and guest species have been omitted for clarity.

Phenanthroline is employed to satisfy the coordination geometry of the Dy^{3+} ions by replacing MBDA in **2**, resulting in tuning of the crystal structures.¹⁰ However, this could also strengthen the magnetic energy barrier. Magnetic susceptibility measurements are carried out for **1** and **2** in an applied dc field of 500 Oe in the temperature range of 1.8–300 K. At room temperature, the χT values for **1** and **2** are 28.11 and 27.93 $\text{cm}^3 \text{K mol}^{-1}$, respectively, which are in good agreement with the expected value of 28.34 $\text{cm}^3 \text{K mol}^{-1}$ for two uncoupled Dy^{3+} ions ($S = 5/2$, $L = 5$, $^6\text{H}_{15/2}$, $g = 4/3$). The χT product remains relatively constant above 70 K before rapidly decreasing at lower temperatures, reaching 20.25 and 19.72 $\text{cm}^3 \text{K mol}^{-1}$ at 2 K for **1** and **2**, respectively. The decline of the χT product is generally indicative of intramolecular anti-ferromagnetic coupling of the metal centers. However, due to the large distance between the Dy^{3+} ions, this behavior is attributed to the thermal depopulation of the Stark sub-level and/or to the presence of large anisotropy in this system. The magnetization plots, M vs. H/T , for **1** and **2** show the field dependence of the magnetization, which does not saturate at low temperature and high magnetic fields. The result reveals the existence of significant magnetoanisotropy and/or low lying excited states.

To study the possible SMM behavior, ac magnetic susceptibility measurements are carried out under zero dc field. No maxima of the characteristic frequency dependence of the out-of-phase signal, χ'' , are found for **1** below 14 K, which is indicative of obvious QTM. Moreover, the SMM behavior of **2** is revealed by the maximum that is detected at 10 K (Fig. 2). Below 4 K, the relaxation of **2** becomes temperature-independent, which is indicative of the quantum regime. Analysis of frequency-dependent data between 9.5 and 12 K using the Arrhenius law [$\tau = \tau_0 \exp(U_{\text{eff}}/k_{\text{B}}T)$, $\tau = 1/2\pi f_{\text{max}}$] gives a

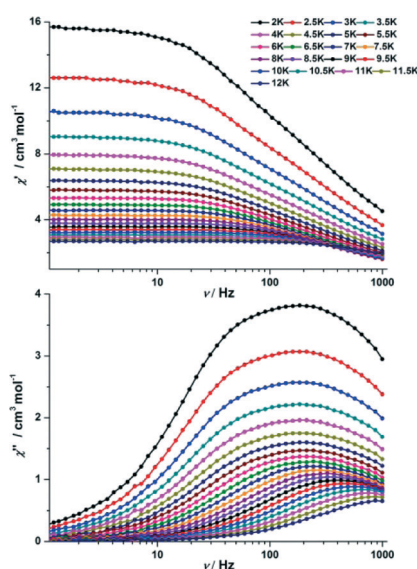


Fig. 2 Frequency dependence of the real (top) and imaginary (bottom) components of the ac magnetic susceptibilities for **2** under zero dc field in the temperature range of 2–12 K.

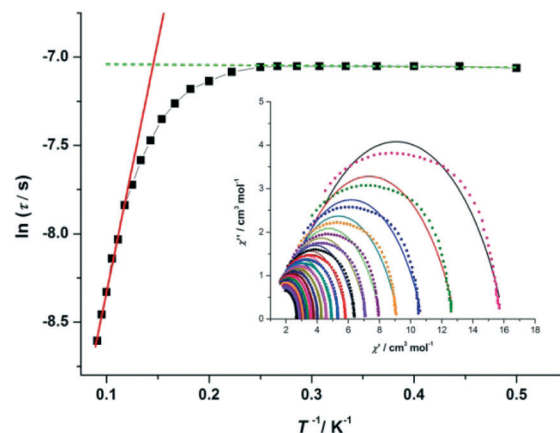


Fig. 3 The relaxation time plotted as $\ln(\tau)$ vs. T^{-1} for **2** under zero dc field. The red line is fitted using the Arrhenius law. The inset shows the Cole-Cole plots of **2** under zero dc field (2–12 K, at intervals of 0.5 K).

relaxation barrier of $U_{\text{eff}} = 28 \text{ K}$ and $\tau_0 = 1.4 \times 10^{-5} \text{ s}$ for **2**. The relatively smaller barrier is ascribed to the presence of QTM (Fig. 3).

To quench the quantum tunnelling effect of **1** and **2**, ac susceptibility measurements as a function of the frequency at different temperatures are carried out under a dc field of 2000 Oe, where the quantum tunnelling is minimized (Fig. 4 and 5). The data plotted as Cole-Cole plots of **1** in the temperature range of 2–12 K show a symmetrical shape and can be fitted to the generalized Debye model.¹⁷ The relaxation time is extracted from the frequency-dependent data in the range of 8–10.5 K and the Arrhenius plot obtained from these data is given in Fig. S16.† Above 8.5 K, the relaxation follows a thermally activated Orbach mechanism with an energy gap

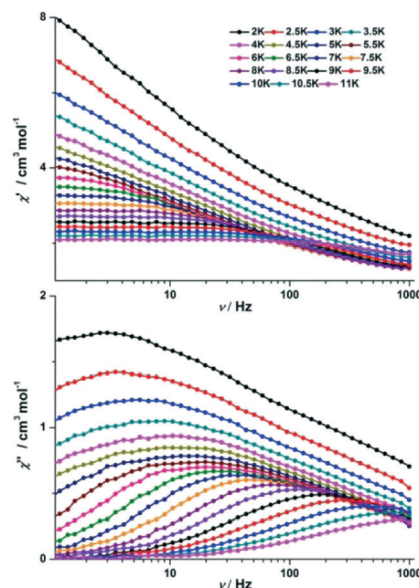


Fig. 4 Frequency dependence of the real (top) and imaginary (bottom) components of the ac magnetic susceptibilities for **1** under an applied field of 2000 Oe in the temperature range of 2–11 K.

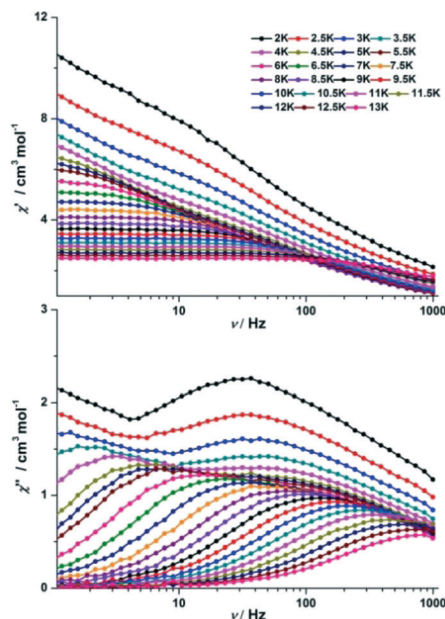


Fig. 5 Frequency dependence of the real (top) and imaginary (bottom) components of the ac magnetic susceptibilities for **2** under an applied field of 2000 Oe in the temperature range of 2–13 K.

of 81 K and a pre-exponential factor τ_0 of 1.0×10^{-7} s. Moreover, the occurrence of two distinct peaks for the out-of-phase ac signals (χ'') is evident at higher frequencies, revealing the possibility of a multiple relaxation process.¹⁸ The Cole–Cole plot of **2** in the temperature range of 2–13 K exhibits a unique double-ridge structure. The anisotropic energy gaps are calculated to be 59 K (1.6×10^{-6} s) and 9 K (3.7×10^{-4} s) for the low temperature and high temperature domains (Fig. S19[†]), respectively. It is noted that the τ_0 values are larger than the expected values for SMM,¹⁹ which is probably enhanced by the presence of QTM.

Conclusions

The crystallization of triple-stranded and quadruple-stranded Dy-based helicates has been achieved through delicate ligand design, with respect to the advantages of weak interactions and the intrinsic geometric elements. The weak but attractive F...F and C–H...F interactions steer the molecular orientation to supramolecular self-assembly. The present study demonstrates the promise of bis- β -diketonate as an excellent chelator for the synthesis of Dy-SMM, while **2** exhibits SMM behavior. Furthermore, it is believed that the 4f-based multiple helicates would be promising candidates for use in separation, catalysis and photocatalysis processes with respect to their chiral nature.

Experimental section

Materials and instrumentation

Elemental analyses were performed on an Elementar Vario EL cube analyzer. FT-IR spectra were obtained on a Perkin-

Elmer Spectrum One spectrophotometer using KBr disks in the range of 4000–370 cm^{-1} . The ^1H NMR spectra were recorded on a Bruker Avance III 400 MHz spectrometer in a DMSO- d_6 solution. Magnetic susceptibility measurements were performed with crystals of **1** and **2** in the temperature range of 2–300 K, using a Quantum Design MPMS-3 SQUID magnetometer equipped with a 7 T magnet. The dc measurements were carried out from 2 to 300 K and the ac measurements were carried out in a 2.0 Oe ac field oscillating at various frequencies from 1 to 1000 Hz and with a zero dc field. The diamagnetic corrections for the compounds were estimated using Pascal's constants and magnetic data were corrected for diamagnetic contributions of the sample holder. MS detection was performed on an Agilent 6520 Q/TOF mass spectrometer with an ESI source and an Agilent G1607A coaxial sprayer (all from Agilent). Thermogravimetric analyses were conducted on an SDT Q600 thermogravimetric analyzer at a heating rate of 20 $^\circ\text{C min}^{-1}$ under air atmosphere in the temperature range of 50–780 $^\circ\text{C}$.

Syntheses

H_2MBDA was synthesized by the Claisen condensation of ethyl trifluoroacetate and *N*-methyl-4,4'-diacetyldiphenylamine in DME (ethylene glycol dimethyl ether). A mixture of sodium methoxide (0.606 g, 11.22 mmol) and ethyl trifluoroacetate (1.328 g, 9.35 mmol) in 30 mL dry DME was stirred for 20 min, followed by the addition of *N*-methyl-4,4'-diacetyldiphenylamine (1.00 g, 3.74 mmol). Then, this mixture was further stirred at room temperature for 24 h. The resulting mixture was poured into 100 mL ice-water and acidified to pH = 2–3 using hydrochloric acid (2 M) and the resulting white precipitate was filtered and dried under vacuum. Recrystallization from acetonitrile gave yellow flake crystals (1.3 g, 77 wt%). Anal. calc. for $\text{C}_{21}\text{H}_{15}\text{F}_6\text{NO}_4$ (459.34): C, 54.91; H, 3.29; N, 3.05 wt%. Found: C, 54.93; H, 3.30; N, 3.05 wt%. IR (KBr, cm^{-1}): 3122 (w), 1582 (s), 1487 (s), 1282 (s), 1202 (s), 1158 (s), 1058 (s), 791 (m), 661 (w), 580 (m). ^1H NMR (400 MHz, DMSO- d_6 , 25 $^\circ\text{C}$, TMS): δ = 8.13 (d, J = 8.88 Hz, 4H), 7.31 (d, J = 8.88 Hz, 4H), 6.95 ppm (s, 2H), 3.50 ppm (s, 3H). ESI-MS m/z : 460.0939 ($\text{M} + \text{H}^+$).

$[\text{C}_6\text{H}_{16}\text{N}]_{3.5}[\text{Dy}_2(\text{MBDA})_4] \cdot 1.5\text{Cl} \cdot 2\text{CH}_3\text{CN} \cdot \text{C}_3\text{H}_6\text{O} \cdot \text{C}_4\text{H}_{10}\text{O}$ (**1**). To a methanol solution (15 mL) of H_2MBDA (0.500 g, 1.089 mmol), triethylamine (0.220 g, 2.2 mmol) and $\text{DyCl}_3 \cdot 6\text{H}_2\text{O}$ (0.199 g, 0.544 mmol) were added and the mixture was stirred for 24 h at room temperature. The precipitate was filtered and dried under vacuum. Single crystals of **1** suitable for single-crystal X-ray diffraction study were obtained by the slow diffusion of diethyl ether into a (0.010 g) $\text{CH}_3\text{CN}/\text{acetone}$ (6 mL/8 mL) solution over 7 days (yield: 35%). Anal. calc. for $\text{C}_{116}\text{H}_{130}\text{Cl}_{1.5}\text{Dy}_2\text{F}_{24}\text{N}_{9.5}\text{O}_{18}$ (2779.47): C, 50.13; H, 4.71; N, 4.79 wt%. Found: C, 50.05; H, 4.63; N, 4.80 wt%.

$[\text{Dy}_2(\text{MBDA})_3(\text{phen})_2] \cdot 0.5\text{CH}_3\text{CN} \cdot \text{C}_3\text{H}_6\text{O} \cdot \text{C}_4\text{H}_{10}\text{O}$ (**2**). A mixture of H_2MBDA (0.500 g, 1.089 mmol) and NaOH (0.087 g, 2.177 mmol) in a methanol solution (15 mL) was stirred for 15 min at room temperature. Then, $\text{DyCl}_3 \cdot 6\text{H}_2\text{O}$ (0.274 g, 0.73

mmol) in methanol solution (10 mL) was added dropwise and the resultant mixture was further stirred for 12 h. Finally, the auxiliary phenanthroline was added into the mixture, and the mixture was refluxed for 4–5 h. The precipitate was filtered and dried under vacuum. Single crystals of 2 suitable for single-crystal X-ray diffraction study were obtained by the slow diffusion of diethyl ether into a (0.010 g) CH₃CN/CHCl₃/acetone (1 mL/6 mL/9 mL) solution over 7 days (yield: 23%). Anal. calc. for C₉₅H_{72.5}Dy₂F₁₈N_{7.5}O₁₄ (2210.10): C, 51.63; H, 3.31; N, 4.75 wt%. Found: C, 51.59; H, 3.22; N, 4.99 wt%.

Acknowledgements

The authors acknowledge financial support from the NSFC (21102039, 21272061, 51102081 and 51302068).

Notes and references

- (a) I. A. Riddell, T. K. Ronson and J. R. Nitschke, *Chem. Sci.*, 2015, **6**, 3533–3537; (b) L. Ungur, S. Lin, J. Tang and L. F. Chibotaru, *Chem. Soc. Rev.*, 2014, **43**, 6894–6905; (c) T. R. Cook, Y. Zheng and P. J. Stang, *Chem. Rev.*, 2013, **113**, 734–777; (d) B. Wang, Z. Zang, H. Wang, W. Dou, X. Tang, W. Liu, Y. Shao, J. Ma, Y. Li and J. Zhou, *Angew. Chem., Int. Ed.*, 2013, **52**, 3756–3759; (e) E. Yashima, K. Maeda, H. Iida, Y. Furusho and K. Nagai, *Chem. Rev.*, 2009, **109**, 6102–6211; (f) J. Xu and K. N. Raymond, *Angew. Chem., Int. Ed.*, 2006, **45**, 6480–6485; (g) C. Piguet and J.-C. G. Bünzli, in *Handbook on the Physics and Chemistry of Rare Earths*, ed. K. A. Gschneidner Jr, J.-C. G. Bünzli and V. K. Pecharsky, Elsevier Science, Amsterdam, 2010, vol. 40, pp. 301–553.
- (a) A. Sørensen, A. M. Castilla, T. K. Ronson, M. Pittelkow and J. R. Nitschke, *Angew. Chem., Int. Ed.*, 2013, **52**, 11273–11277; (b) J.-C. G. Bünzli, *Interface Focus*, 2013, **3**, 20130032; (c) W. Xuan, M. Zhang, Y. Liu, Z. Chen and Y. Cui, *J. Am. Chem. Soc.*, 2012, **134**, 6904–6907; (d) M. J. Hannon, *Chem. Soc. Rev.*, 2007, **36**, 280–295; (e) M. Albrecht, *Chem. Rev.*, 2001, **101**, 3457–3497; (f) C. Piguet, G. Bernardinelli and G. Hopfgartner, *Chem. Rev.*, 1997, **97**, 2005–2062.
- (a) F. Habib, J. Long, P. Lin, I. Korobkov, L. Ungur, W. Wernsdorfer, L. F. Chibotaru and M. Murugesu, *Chem. Sci.*, 2012, **3**, 2158–2164; (b) E. Terazzi, L. Guénée, J. Varin, B. Bocquet, J. F. Lemonnier, D. Emery, J. Mareda and C. Piguet, *Chem. – Eur. J.*, 2011, **17**, 184–195.
- (a) Y. Shu, X. Tang and W. Liu, *Inorg. Chem. Front.*, 2014, **1**, 226–230; (b) F. Stomeo, C. Lincheneau, J. P. Leonard, J. E. O'Brien, R. D. Peacock, C. P. McCoy and T. Gunnlaugsson, *J. Am. Chem. Soc.*, 2011, **131**, 9636–9637; (c) B. E. Aroussi, S. Zebret, C. Besnard, P. Perrottet and J. Hamacek, *J. Am. Chem. Soc.*, 2011, **133**, 10764–10767; (d) J. Jiang, S. Zheng, Y. Liu, M. Pan, W. Wang and C. Su, *Inorg. Chem.*, 2008, **47**, 10692–10699; (e) K. Zeckert, J. Hamacek, J. Senegas, N. Dalla-Favera, S. Floquet, G. Bernardinelli and C. Piguet, *Angew. Chem., Int. Ed.*, 2005, **44**, 7954–7958; (f) J. Yuan, S. Sueda, R. Somazawa, K. Masumoto and K. Matsumoto, *Chem. Lett.*, 2003, **32**, 492–493.
- (a) P. E. Ryan, L. Guenee and C. Piguet, *Dalton Trans.*, 2013, **42**, 11047–11055; (b) J.-C. G. Bünzli, *Chem. Rev.*, 2010, **110**, 2729–2755; (c) M. Albrecht, O. Osetska, J.-C. G. Bünzli, F. Gumy and R. Frohlich, *Chem. – Eur. J.*, 2009, **15**, 8791–8799; (d) A.-S. Chauvin, S. Comby, B. Song, C. D. B. Vandevyver, F. Thomas and J.-C. G. Bünzli, *Chem. – Eur. J.*, 2007, **13**, 9515–9526; (e) M. Elhabiri, R. Scopelliti, J.-C. G. Bünzli and C. Piguet, *J. Am. Chem. Soc.*, 1999, **121**, 10747–10762.
- A. P. Bassett, S. W. Magennis, P. B. Glover, D. J. Lewis, N. Spencer, S. Parsons, R. M. Williams, L. D. Cola and Z. Pikramenou, *J. Am. Chem. Soc.*, 2004, **126**, 9413–9424.
- (a) A. M. Johnson, M. C. Young, X. Zhang, R. R. Julian and R. J. Hooley, *J. Am. Chem. Soc.*, 2013, **135**, 17723–17726; (b) J. Hamacek, C. Besnard, T. Penhouet and P.-Y. Morgantini, *Chem. – Eur. J.*, 2011, **17**, 6753–6754; (c) B. E. Aroussi, S. Zebret, C. Besnard, P. Perrottet and J. Hamacek, *J. Am. Chem. Soc.*, 2011, **133**, 10764–10767.
- (a) T. Zhu, P. Chen, H. Li, W. Sun, T. Gao and P. Yan, *Phys. Chem. Chem. Phys.*, 2015, **17**, 16136–16144; (b) H. Li, P. Yan, P. Chen, Y. Wang, H. Xu and G. Li, *Dalton Trans.*, 2012, **41**, 900–907; (c) H. Li, G. Li, P. Chen, W. Sun and P. Yan, *Spectrochim. Acta, Part A*, 2012, **97**, 197–201.
- (a) J. Leng, H. Li, P. Chen, W. Sun, T. Gao and P. Yan, *Dalton Trans.*, 2014, **43**, 12228–12235; (b) P. He, H. H. Wang, S. G. Liu, J. X. Shi, G. Wang and M. L. Gong, *Inorg. Chem.*, 2009, **48**, 11382–11387.
- (a) G. Chen, Y. Guo, J. Tian, J. Tang, W. Gu, X. Liu, S. Yan, P. Cheng and D. Liao, *Chem. – Eur. J.*, 2012, **18**, 2484–2487; (b) Y. Bi, Y. Guo, L. Zhao, Y. Guo, S. Lin, S. Jiang, J. Tang, B. Wang and S. Gao, *Chem. – Eur. J.*, 2011, **17**, 12476–12481.
- (a) R. Zhu, J. Lübben, B. Dittrich and G. H. Clever, *Angew. Chem., Int. Ed.*, 2015, **54**, 2796–2800; (b) W. Colson and W. R. Dichtel, *Nat. Chem.*, 2013, **5**, 453–465; (c) K. Chadwick, J. Chen, A. S. Myerson and B. L. Trout, *Cryst. Growth Des.*, 2012, **12**, 1159–1166; (d) Y. Chang, Z. Lu, L. An and J. Zhang, *J. Phys. Chem. C*, 2012, **116**, 1195–1199.
- (a) M. D. Ward and P. R. Raithby, *Chem. Soc. Rev.*, 2013, **42**, 1619–1636; (b) M. D. Pluth, R. G. Bergman and K. N. Raymond, *J. Am. Chem. Soc.*, 2009, **131**, 1650–1659.
- B. Wu, S. Li, Y. Lei, H. Hu, N. D. S. Amadeu, C. Janiak, J. S. Mathieson, D. Long, L. Cronin and X. Yang, *Chem. – Eur. J.*, 2015, **21**, 2588–2593.
- (a) R. Berger, G. Resnati, P. Metrangolo, E. Weber and J. Hulliger, *Chem. Soc. Rev.*, 2011, **40**, 3496–3508; (b) D. Chopra and T. N. G. Row, *CrystEngComm*, 2011, **13**, 2175–2186; (c) A. Schwarzer, P. Bombicz and E. Weber, *J. Fluorine Chem.*, 2010, **131**, 345–356.
- (a) A. Putta, J. D. Mottishaw, Z. Wang and H. Sun, *Cryst. Growth Des.*, 2014, **14**, 350–356; (b) M. Podsiadlo, A. Olenjniczak and A. Katrusiak, *CrystEngComm*, 2014, **16**, 8279–8285; (c) S. Sirimulla, J. B. Bailey, R. Vegesna and M. Narayan, *J. Chem. Inf. Model.*, 2013, **53**, 2781–2791.
- (a) A. J. Cruz-Cabeza and J. Bernstein, *Chem. Rev.*, 2014, **114**, 2170–2191; (b) A. Nangia, *Acc. Chem. Res.*, 2008, **41**, 595–604.

- 17 S. M. J. Aubin, Z. Sun, L. Pardi, J. Krzystek, K. Folting, L. C. Brunel, A. L. Rheingold, G. Christou and D. N. Hendrickson, *Inorg. Chem.*, 1999, **38**, 5329–5340.
- 18 Y. Guo, G. Xu, P. Gamez, L. Zhao, S. Lin, R. Deng, J. Tang and H. Zhang, *J. Am. Chem. Soc.*, 2010, **132**, 8538–8539.
- 19 (a) Y. Gao, G. Xu, L. Zhao, J. Tang and Z. Liu, *Inorg. Chem.*, 2009, **48**, 11495–11497; (b) F. Tuna, C. A. Smith, M. Bodensteiner, L. Ungur, L. F. Chibotaru, E. J. L. McInnes, R. E. P. Winpenny, D. Collison and R. A. Layfield, *Angew. Chem., Int. Ed.*, 2012, **51**, 6976–6980; (c) F. Pointillart, S. Klementieva, V. Kuropatov, Y. L. Gal, S. Golhen, O. Cadot, V. Cherkasov and L. Ouahab, *Chem. Commun.*, 2012, **48**, 714–716.